

ZnS, ZnSe and ZnTe (110) Surfaces: Atomic Structures and Electronic Properties

J. L. A. Alves*, K. Watari and A. C. Ferraz

Instituto de Física, Universidade de São Paulo

Caixa Postal 20.516, CEP 01498-970, São Paulo, SP, Brasil

Received August 27, 1993; revised manuscript received October 25, 1993

In this paper we describe a systematic study of the atomic and electronic properties of ZnS, ZnSe and ZnTe (110) surfaces. We analyze the trends for the equilibrium atomic structures, photoelectric thresholds and surface band structure where the latter two properties have recently been object of experimental angular-resolved photoemission studies. We report calculations which are based on the density-functional theory, the local-density approximation for the exchange-correlation function and the self-consistent ab-initio pseudopotentials. The surface's layers were relaxed according to the forces on atoms, using an "optimized steepest descent" method together with a Car-Parrinello approach.

I. Introduction

Compared to 111-V semiconductor surfaces, the knowledge of the electronic structure of 11-VI semiconductors is scarce. In fact, few experiments using angle-resolved photoelectron spectroscopy have been done^[1] and a major obstacle is the problem of identifying the surface-derived spectral features. In particular, photoemission from band edges may in many cases be difficult to distinguish from surface-state emission. A more recent study of ZnSe (110) and ZnTe (110)^[2] has revealed several features in the photoelectron spectra which were associated with the surface states and surface resonances different from that of Ref. [1]. It is noted, however, that the energy position of the surface states, particularly of the state lying near the forbidden gap edge, is sensitive to the position of the surface atoms^[3,4]. On the other hand, low-energy electron diffraction (LEED) is the technique most frequently used to establish the atomic structure of semiconductor surfaces, although isochromat spectroscopy, ion-scattering and surface-extended x-ray-absorption fine structure (SEXAFS) techniques are also often applied. From these results a common reconstruction pattern of

the 111-V and 11-VI surface has been established: at the surface the anion moves away from the bulk towards a pyramidal geometry (the average bond angle at the anion is around 95°), whereas the cation moves into the bulk towards a planar geometry (bond angles close to 120°)^[1,5]. The relative displacement of the cation and the anion within the outermost layer defines a rotation angle ω which is generally believed to play a unique role in characterizing this reconstruction pattern.

In this paper we report results of ab-initio, self-consistent pseudopotential calculations based on the density-functional theory^[6,7] applying the local-density approximation^[8,9]. We study the ZnS(110), ZnSe(110) and ZnTe(110) surfaces and analyze the trends for the equilibrium atomic structures, photoelectric thresholds, and surface band structures.

II. Method and atomic geometry

We present results of first-principle, self-consistent density-functional theory^[6,7] calculations for electronic structure, total energy and force. Electron-ion interaction was treated by using norm-conserving pseudopotentials in the Kleinman-Bylander form^[10,11] and the electronic exchange-correlation functional was related

*Present address: Fundação de Ensino Superior de São João del Rei, DCNAT, Caixa Postal 110, São João Del Rei, MG, Brasil

within the local-density approximation by using the Ceperley-Alder scheme^[8,9].

We use the repeated-slab method^[12] to simulate the semiconductor surface. The system is periodic parallel to the surface and we introduce an artificial periodicity perpendicular to the surface, defining a large three-dimensional unit cell. Our slab contains eight (110) layers of II-VI compounds plus a vacuum region of six inter-layers distances.

In order to determine the equilibrium atomic positions for the surface calculations the three outermost layers on both sides of the slab were relaxed to the geometry given by the calculation of the total energy and forces using an "optimized steepest descent" method for the atomic displacements together with a Car-Parrinello^[13] approach for bringing the wave functions to self-consistency. To simulate the molecular dynamics we followed a trajectory on a fictitious energy surface and achieved a simultaneous relaxation of the electronic and ionic degrees of freedom by treating the ionic coordinates and the electronic wave functions for occupied states as dynamical degrees of freedom of a fictitious system. The fictitious electron dynamics was simulated by assigning a fictitious mass to the single-particle electron wave functions. This fictitious mass was adjusted so that the ions remained close to the Born-Oppenheimer surface, and a periodic electronic minimization was performed.

The equilibrium geometry is identified when all forces are smaller than 0.005eV/Å corresponding to a numerical uncertainty of the atomic positions of less than 0.05Å. The single-particle wave functions were expanded in plane waves up to a kinetic energy of 10 Ry and the summation over four Monkhorst-Pack^[14] k points in the irreducible part of the surface Brillouin Zone was used to replace the Brillouin Zone integrations. The equations of motion for the Fourier coefficients of the plane waves were solved by using the steepest descent algorithm of Payne et al.^[15], and the ion dynamics was performed by using a damped Verlet

algorithm^[16]

The lattice constants are fixed at the bulk theoretical equilibrium values and are given for the three systems in Table I. The theoretical lattice constants are about 7% smaller than the experimental ones for ZnS and ZnSe, and about 4% for ZnTe. These discrepancies are to be attributed to the missing contribution of the Zn 3d states which are considered as frozen core states and thus hidden in the pseudopotentials. Since our main interest is in the changes which occur at the II-VI (110) surfaces we generated a pseudopotential of a zinc atom by regarding its 3d orbitals as core orbitals and by choosing suitable core radii and an electron configuration $s^x p^y$ which is able to reproduce the experimental bulk structural constants within minor errors.

Schematically the relaxation is shown in Fig. 1, which also defines the structural parameters in Table I and II. The relaxed surfaces are on a such way that the group II surface atom moves inward and the group VI moves outward. The driving mechanism for this atomic rearrangement is similar to 111-L' (110) surfaces^[17]: under the coordination conditions of the surface, the group II atom prefers a more planar, sp^2 -like bonding situation with its three group VI neighbors and the group VI atom prefers a p-bonding with its three group II neighbors.

Our results for the structural parameters and the results of low-energy electron diffraction (LEED) analysis^[18] are shown in Table I. The II-VI (110) surfaces relaxation with the surface cations moving inward and the surface anions outward has revealed the LEED results and was reproduced by our calculations. The most accurately structural parameter determined by LEED intensity analysis is the relative displacement $\Delta_{1,1}$ and our calculated values for that parameter are systematically smaller than the experimentally derived ones. The calculated tilt angles (ω) are in good agreement with the experimental values, which are determined with a precision of 10%.

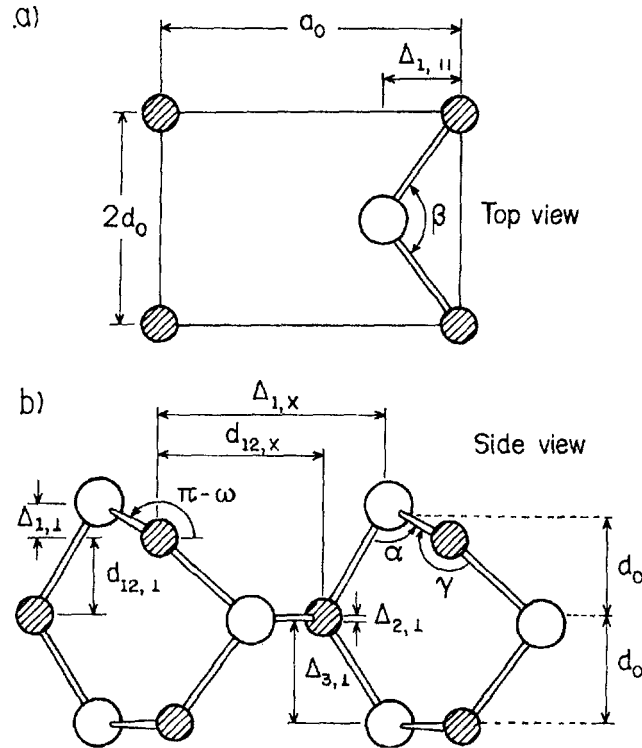


Figure 1: Atomic geometry for II-VI semiconductor (110) surfaces. (a) Top view of the surface unit cell. (b) Side view of the first three layers of the (110) surface. Open circles are anions and hatched circles are cations. a_0 is the theoretical bulk lattice constant and $d_0 = \sqrt{2}a_0/4$.

Table I - Structural parameters for the surface relaxation as defined in Fig. 1. For each compound the first line corresponds to the LEED analysis^[18].

	a_0 (Å)	$\Delta_{1,\perp}$ (Å)	$\Delta_{1,\parallel}$ (Å)	$\Delta_{2,\perp}$ (Å)	$d_{12,L}$ (Å)	$d_{23,\perp}$ (Å)	$d_{12,V}$ (Å)	ω (°)
ZnS	5.410	0.59	4.19	0.00	1.53	1.91	3.15	26.0
	5.027	0.43	4.05	0.07	1.33	1.84	2.84	23.9
ZnSe	5.668	0.69	4.43	0.00	1.52	2.00	3.35	29.0
	5.259	0.50	4.21	0.07	1.39	1.91	2.98	25.4
ZnTe	6.104	0.72	4.75	0.00	1.64	2.15	3.59	28.5
	5.883	0.63	4.72	0.09	1.47	2.13	3.36	28.4

Table II. Calculated tilt angle ω , relative displacement $\Delta_{1,\perp}$ in % of lattice constant a_0 , bond-angles at the anions and at the cations located at the first layer, and $Z e^2 / \epsilon_0 a_0$ in eV.

	ω (°)	$\Delta_{1,\perp} a_0$ (%)	α (°)	β (°)	γ (°)	$Z e^2 / \epsilon_0 a_0$ (eV)
GaP	27.8	10.6	92.3	114.1	122.0	0.442
GaAs	28.6	11.4	90.8	112.1	122.3	0.255
InP	29.2	11.3	91.4	113.7	122.4	0.582
InAs	30.7	12.0	90.1	112.5	123.3	0.235
ZnS	23.9	8.5	95.6	119.4	117.9	1.809
ZnSe	25.4	9.5	94.2	120.6	116.0	1.225
ZnTe	28.4	10.7	92.4	121.8	115.1	0.924

In Table II we display the bond angles obtained in our present calculation for the II-VI (110) surfaces together with the angles obtained for the III-V (110) surfaces in reference^[17]. The angle α is bigger in II-VI compounds than in III-V compounds. On the other hand the angle α is closer to 90° as one goes from phosphorus compound to arsenic compound in III-V compounds (e.g. from GaP to GaAs) or from sulphur compound to selenium and then to tellurium compound in II-VI compounds. Besides the influence of the repulsion between the chemical bonds, one has to take into account the ionic character of these bonds, which increases from III-V to II-VI compounds. The Phillips ionicities^[19] for GaP, GaAs, InP, InAs, ZnS, ZnSe and ZnTe are 0.374, 0.310, 0.421, 0.357, 0.023, 0.676 and 0.576, respectively. For the more ionic zinc-blende semiconductors, the attractive Coulomb forces between the outward relaxed surface anions and the inward relaxed surface cations should reduce the relaxation caused by covalent forces. In Table II we compare the trends of the angle α and the Coulomb energy $Ze^2/\epsilon a_0$, where a_0 is the theoretical lattice constant, Z is the longitudinal effective charge, e is the electron's charge and ϵ is the dielectric constant^[20,21]. The ionicity is approximately proportional to Z ^[22]. As shown in Table II, for compounds with a common cation the angle α decreases, getting closer to 90° , when the Coulomb energy decreases. Moreover this fact is reflected in the trend of the calculated tilt angle ω , which increases when the Coulomb energy decreases. It is worth noting that the calculated relative displacement $\Delta_{1,\perp}$ in % of the theoretical lattice constant a_0 is smaller for higher Coulomb energies.

Although smaller than the relaxation of the III-V (110) surfaces due to the competition between covalent and ionic forces, the relaxation of II-VI (110) surfaces is driven by the same mechanism: the group VI atom tends to p -bonding with its three group II neighbors, forming a pyramidal geometry^[23]. On the other

Table III. Photothresholds of II-VI semiconductor compounds in units of eV.

ZnS	ZnSe	ZnTe	
7.50	6.82	5.76	Expt(ref.25)
6.40	6.11	5.46	theory

way, our calculations are sensitive to the ionicity of the materials and the results are in good agreement with previous arguments which predict that the relaxation angle ω of zinc-blend (110) surfaces should depend on ionicity^[20,21]. Apparently the LEED analysis are not sensible enough to the ionicity of the systems since they give about the same value $\omega \cong 28^\circ$ for all zinc-blend (110) surfaces.

III. Band structures

The photoelectric threshold is the minimum energy required to remove one electron from the valence band, so it is the energy difference between the vacuum level and the valence-band maximum. We follow the procedure of Ref. [24] to calculate this energy by combining bulk and surface calculation. In the bulk calculation the top of the valence band is determined relative to the bulk potential and in the surface calculation the vacuum level is determined relative to the bulk potential. Our results for the photoelectric threshold relative to the II-VI compounds are shown in Table III. Again the ionicity makes the rule and the photothreshold is decreased with increasing ionicity in agreement with the experimental trend. The difference between the experimental value and the calculated value is a measure of how much the eigenvalues on the density-functional theory with local-density approximation deviates from the true quasiparticle excitations, and it is due partly to the neglect of the d orbitals in Zn as valence states.

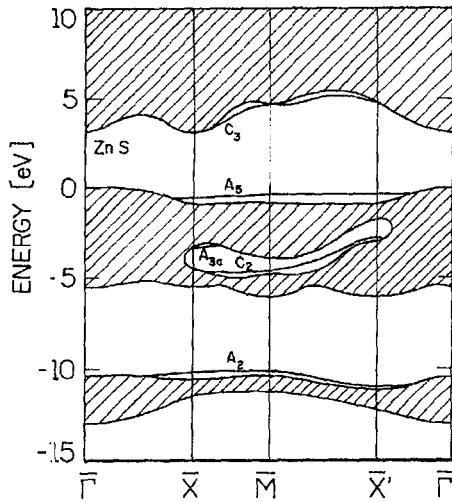


Figure 2: Energy dispersion of surface states on the ZnS (110) surface

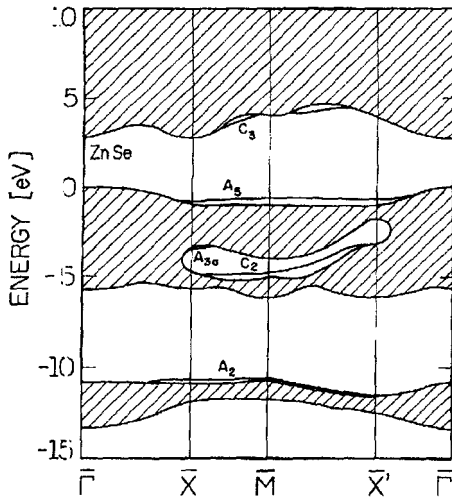


Figure 3: Energy dispersion of surface states on the ZnSe (110) surface.

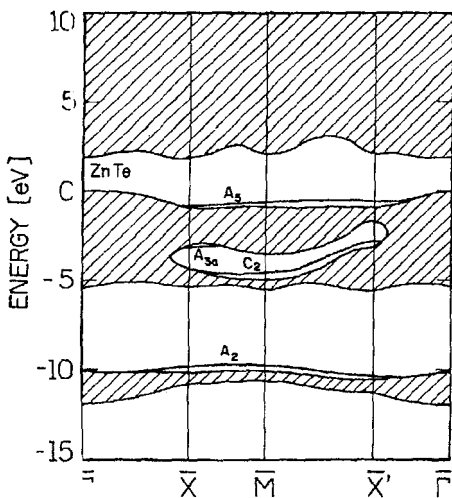


Figure 4: Energy dispersion of surface states on the ZnTe (110) surface.

The calculated (110) surface band structures of ZnS, ZnSe and ZnTe are shown in Figs. 2-4 along the prime-

ter $\bar{\Gamma} \text{ X } \bar{M} \text{ X}' \bar{\Gamma}$ of the surface Brillouin zone. The hatched region indicates the projected bulk band structure and the solid lines represent the bound surface states. The cation and anion derived surface states are labelled as C_i and A_i , respectively.

The common features to all surface electronic states are as follows:

a) The state A_2 lies in the antisymmetric gap and its position and dispersion do not change much between the compounds. It is derived from the s orbital of the top layer anions lying around -10.0 and -11.0 eV.

b) There are surface states A_3 (p_x -like) and C_2 (s -like) lying in the central region of the bulk valence bands (stomach gap) and localized on anion atoms in the second layer and on Zn atoms in the first layer. As the state A_2 , these states do not change between the compounds.

c) There are surface states in the fundamental gap between the valence band and the conduction band arising from both the empty cation-derived dangling bond C_3 and the occupied anion-derived dangling bond A_5 states. C_3 is derived from a mixture of s and p , orbitals of the top layer cations (Zn) and lies quite close to its lower edge near the conduction band minimum around $\text{X } \bar{M} \text{ X}'$ points of the surface Brillouin Zone. A_5 is derived from the p , orbital of the top layer anions and lies flat at about 0.5 eV down the bulk valence band maximum around $\text{X } \bar{M} \text{ X}'$ points of the surface Brillouin Zone.

d) Increasing the ionicity (from ZnS to ZnTe) the state C_3 is shifted to the bulk minimum conduction band, becoming a gap free of C_3 state.

Our results are qualitatively in agreement with few other theoretical findings of previous slab (110) 11-VI surface calculations. These earlier calculations used empirical tight-binding^[26,27] or pseudopotentials methods^[28]. The main difference between our calculations and the previous ones is related to the A_5 state. While on that calculations the state lies flat and in the

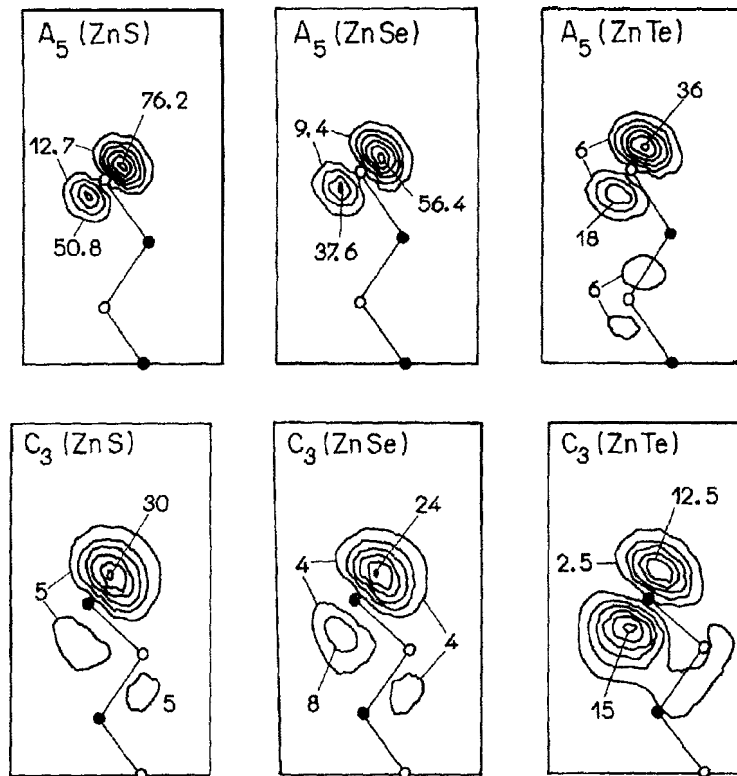


Figure 5: Electronic charge density contour plots for A_5 and C_3 surface states at the middle k point between \bar{M} and \bar{X}' . Open circles indicate the anions and the solid circles indicate the cations. Units are $10^{-3} \text{ bohr}^{-3}$.

gap along all the surface Brillouin Zone, in our results A_5 lies in the gap only between \bar{X} \bar{M} \bar{X}' points and is closer to the top of valence band. That deeper A_5 state agree very well with the recent angle-resolved photoelectron spectroscopy study^[2] but with different feature from that of Ebina et al.^[1] on older angle-resolved spectra, where A_5 lies almost flat in the gap along all the surface Brillouin Zone.

In Fig. 5 we display the anion and cation dangling-bond states (A_5 and C_3) through charge density plots for the 11-VI studied compounds. The A_5 is an occupied bond band whereas the C_3 is an unoccupied bond band. All the anion states look like p states at the surface atoms reducing their density maxima from ZnS to ZnTe where there is some sp^3 -hybrid component at the anion in the third layer. The cation dangling-bond states are more extended, reflecting a strong mixing of s and p orbitals, increasing the mixing from ZnS to ZnTe, and their density maxima are smaller compared to the anion dangling-bond states.

References

1. A. Ebina, T. Unno, Y. Suda., H. Koinuma and T. Takahashi, J. Vac. Sci. Technol. 19, 301 (1981); T. Takahashi and A. Ebina, Appl. Surf. Sci. 11/12, 268 (1982).
2. H. Qu, J. Kanski, P. O. Nilsson and U. O. Karlsson, Phys. Rev. B43, 9843 (1991); 44, 1762 (1991).
3. A. Kahn, Surface Sci. Rept. 3, 193 (1983).
4. A. C. Ferraz and G. P. Srivastava, Surface Sci. 182, 161 (1987).
5. R. Chang and W. A. Goddard III, Surface Sci. 144, 311 (1984).
6. P. Hohenberg and W. Kohn, Phys. Rev. 136, R864 (1964).
7. W. Kohn and L. J. Sham, Phys. Rev. 140, A1133 (1965).
8. D. M. Ceperley and B. I. Alder, Phys. Rev. Lett. 45, 566 (1980).
9. J. P. Perdew and A. Zunger, Phys. Rev. B23, 5048 (1981).
10. L. Kleinman and D. M. Bylander, Phys. Rev. Lett. 48, 1425 (1982).

11. X. Gonze, R. Stumpf and M. Schliefner, Phys. Rev. B44, 8503 (1991).
12. M. Schlüter, J. R. Chelikowsky, S. G. Louie and M. L. Cohen, Phys. Rev. B12, 4200 (1975).
13. R. Car and M. Parrinello, Phys. Rev. Lett. 55, 2471 (1985).
14. H. J. Monkhorst and J. D. Pack, Phys. Rev. B13, 5188 (1976).
15. M. C. Payne, J. D. Joannopoulos, D. C. Allan, M. P. Teter and D. H. Vanderbilt, Phys. Rev. Lett. 56, 2656 (1986).
16. L. Verlet, Phys. Rev. 159, 98 (1967).
17. J. L. A. Alves, J. Hebenstreit and M. Schliefner, Phys. Rev. B44, 6188 (1991).
18. C. B. Duke, *Surface Properties of Electronic Materials*, D. A. King and D. P. Woodruff edited (Elsevier, Amsterdam, 1986) Chap. 3.
19. F. Bechstedt and R. Enderlein, *Semiconductor Surfaces and Interfaces* (Academic Verlag, Berlin, 1988).
20. R. V. Kasowski, M.-H. Tsai and J. D. Dow, J. Vac. Sci. Technol. 85, 953 (1987).
21. M.-H. Tsai, R. V. Kasowski and J. D. Dow, Solid State Commun. 64, 231 (1987).
22. G. Lucovsky, R. M. Martin and E. Burstein, Phys. Rev. B4, 1367 (1971).
23. D. A. Dixon and D. S. Marynick, J. Am. Chem. Soc. 99, 6101 (1977); J. Chem. Phys. 71, 2860 (1979).
24. Guo-Xin Qian, R. M. Martin and D. J. Chadi, Phys. Rev. B37, 1303 (1988).
25. J. van Laar, A. Huijser and T. L. van Rooy, J. Vac. Sci. Technol. 14, 894 (1977).
26. R. P. Beres, R. E. Allen, and J. D. Dow, Phys. Rev. B26, 769 (1982).
27. C. Mailhot, C. B. Duke, and Y. C. Chang, Phys. Rev. B30, 1109 (1984).
28. A. C. Ferraz and G. P. Srivastava, J. Phys. C.19, 5987 (1987).